



## UvA-DARE (Digital Academic Repository)

### Experimental investigation of potential topological and p-wave superconductors

Trần, V.B.

**Publication date**  
2014

[Link to publication](#)

#### **Citation for published version (APA):**

Trần, V. B. (2014). *Experimental investigation of potential topological and p-wave superconductors*. [Thesis, fully internal, Universiteit van Amsterdam].

#### **General rights**

It is not permitted to download or to forward/distribute the text or part of it without the consent of the author(s) and/or copyright holder(s), other than for strictly personal, individual use, unless the work is under an open content license (like Creative Commons).

#### **Disclaimer/Complaints regulations**

If you believe that digital publication of certain material infringes any of your rights or (privacy) interests, please let the Library know, stating your reasons. In case of a legitimate complaint, the Library will make the material inaccessible and/or remove it from the website. Please Ask the Library: <https://uba.uva.nl/en/contact>, or a letter to: Library of the University of Amsterdam, Secretariat, Singel 425, 1012 WP Amsterdam, The Netherlands. You will be contacted as soon as possible.

# Experimental Chapter 2 background and techniques

---

---

*In this chapter, we present a concise description of the experimental techniques used throughout this thesis: sample preparation and characterization, cryogenic techniques and measurement equipment. In addition, we report the calibration of the RuO<sub>2</sub> thermometer in high magnetic field, as well as of the hybrid piston cylinder pressure cell.*

## 2.1 Sample preparation

All samples used in this thesis were fabricated at the WZI by Dr. Y. K. Huang, except some of the YPtBi batches that were synthesized by Dr. T. Orvis at Stony Brook University. Single crystalline  $\text{Cu}_x\text{Bi}_2\text{Se}_3$  samples were prepared by a melting method. A flux technique was applied to synthesize YPtBi single crystals. For UCoGe, polycrystals were synthesized first in a home-built mono-arc furnace. Next, single crystals were grown using the Czochralski method in a tri-arc furnace. The details of the sample preparation processes are given in each experimental chapter.

## 2.2 Sample characterization

Sample characterization is essential prior to making further investigations. This can be accomplished by using various facilities at the WZI. In this work, for instance, X-ray powder diffraction, X-ray back-scattering Laue diffraction and Electron Probe Micro Analysis (EPMA) have been used to investigate in particular sample homogeneity, stoichiometry as well as to identify crystal structures and crystal orientation. In addition, depending on the experimental needs the samples were cut into the desired shapes and dimensions using a spark erosion machine.

## 2.3 Cryogenic techniques

A majority of this PhD work has been done using several low temperature facilities at the WZI. Each system is briefly described in the following paragraphs:

A home-made  $^4\text{He}$  bath cryostat using liquid helium and liquid nitrogen can be operated in the temperature range 1.5-300 K. The base temperature can be reached rapidly by directly reducing the vapour pressure of liquid  $^4\text{He}$  using a rotary pump. This equipment is suitable for initial transport and magnetic measurements such as fast checking of superconductivity and magnetic transitions.

A Maglab Exa cryostat (Oxford Instruments) is used in the temperature range 1.2-400 K. It is equipped with a 9 T superconducting magnet. This cryostat can be used for electrical and ac- and dc-magnetization measurements.

A  $^3\text{He}$  refrigerator, Heliox VL (Oxford Instruments) [1], is operated in the temperature range 0.23-20 K and is equipped with a 14 T superconducting magnet. Its basic principle of operation is based on the property of  $^3\text{He}$  as follows. Liquid  $^3\text{He}$  can be collected in the  $^3\text{He}$  pot by condensing the  $^3\text{He}$  gas with help of the 1 K plate which is cooled by the 1 K pot. The

vapour of the  $^3\text{He}$  is reduced by a sorb pump operated at 4.2 K. Consequently the base temperature (230 mK) is achieved at the  $^3\text{He}$  pot. A multipurpose sample holder is located 20 cm below the  $^3\text{He}$  pot in the center of the magnetic field, and is in good thermal contact with the  $^3\text{He}$  pot. The thermal link is provided by a low eddy current sample holder made of a stainless steel rod that contains sintered copper. The Heliox has a cooling power of  $40\ \mu\text{W}$  at 300 mK. The temperature is controlled by a  $\text{RuO}_2$  thermometer and a heater made of two  $100\ \Omega$  resistors in series. Both the thermometer and the heater are connected to a temperature controller (ITC 503, Oxford Instruments). An additional calibrated thermometer was mounted on the sample platform and read out by an ORPX resistance bridge (Barras Provence). The Heliox is a multi-purpose cryostat for measurements of resistivity, magnetoresistivity, ac-susceptibility, thermal expansion and magnetostriction.

A  $^3\text{He}/^4\text{He}$  dilution refrigerator, Kelvinox MX100 (Oxford Instruments) [2], is operated in the temperature range 0.02-1.2 K and magnetic field range up to 18 T. The cooling mechanism of the Kelvinox basically relies on the temperature-concentration phase diagram of a  $^3\text{He}/^4\text{He}$  mixture. When the mixture is cooled to below 900 mK, it separates into two phases. The lighter ‘concentrated phase’ with almost pure liquid  $^3\text{He}$  is floating on top of the heavier ‘dilute phase’ of superfluid  $^4\text{He}$  with about 6%  $^3\text{He}$ . By pumping on the  $^3\text{He}$  in the dilute phase,  $^3\text{He}$  atoms ‘evaporate’ from the pure phase into the dilute phase, as a result of the osmotic pressure. A base temperature as low as 20 mK is achievable in the mixing chamber. For continuous cooling, over a period of even months, the  $^3\text{He}$  gas is circulated and condensed again at  $\sim 1.2$  K in the 1 K pot. The SC magnet is equipped with a field compensation coil which results in a field smaller than 100 Gauss at the level of the mixing chamber. This prevents eddy current heating of the mixing chamber during field sweeps, and in addition allows for calibration of thermometers in field (see below). The sample holder configuration is like in the Heliox. Moreover, the Kelvinox is equipped with a plastic Swedish rotator with angles tunable from  $-150^\circ$  to  $150^\circ$  with a resolution of  $0.2^\circ$ , controlled by an Oxford Instruments Stepper Motor Control Unit model (SMC4). The Kelvinox’s cooling power is  $100\ \mu\text{W}$  at 100 mK. This is a multi-purpose cryostat like the Heliox, but angular dependence measurements can be performed as well.

In addition, low temperature facilities, including a SQUID at the Néel Institute in Grenoble, France, and a dilution refrigerator at the Paul Scherrer Institute (PSI) in Villigen, Switzerland, have been used. More details about these experimental set-ups can be found in Refs. 3,4,5.

## 2.4 Calibration of RuO<sub>2</sub> thermometers in high magnetic field

Normally the calibration of commercial RuO<sub>2</sub> thermometers is made in zero magnetic field. However, many experiments are carried out in high magnetic fields. Therefore, it is essential to take into account the effect of the magnetic field on the thermometers, and their calibration in field is desirable. This is especially required for the experiments in the Kelvinox. We have done the calibration as follows. We record a resistance value  $R$  of an uncalibrated RuO<sub>2</sub> at the field position and temperature  $T$  of a reference thermometer which is kept in the zero field region at a given set point of temperature and magnetic field when their thermal equilibrium is established. Repeating the same measurement for different temperatures in a magnetic field  $B$  one gets a data set of  $R$ ,  $T$  and hence a function  $T = f(R)$ . If we redo the sequence for different magnetic fields, we obtain  $T = f(R, B)$ . The functions best fitted to the data are listed in the table below. Finally, we establish an average function  $T = f(R, B)$  for the calibration

$$T [K] \Big|_{B=4(m-1)+n} = f_{4(m-1)} + n \frac{|f_{4m} - f_{4(m-1)}|}{4}; \quad m = 1, 2, 3, 4; \quad n = 0, 1, 2, 3, \quad (2.1)$$

where  $B$  is magnetic field, and  $f$  is a function taken from the table at a corresponding field. Thus, the equation (2.1) allows us to calculate the temperature of the thermometer in a magnetic field.

Magnetic field (T)	$T_{\text{RuO}_2}$ (K); $x = R_{\text{RuO}_2}$ (k $\Omega$ )
B = 0	$f_0 = y_0 + a_1 e^{-(x-x_0)/t_1} + a_2 e^{-(x-x_0)/t_2} + a_3 e^{-(x-x_0)/t_3}$ $y_0 = 0.006822972; x_0 = 6.086899996$ $a_1 = 0.205591216; a_2 = 0.590778143; a_3 = 0.373789468$ $t_1 = 4.904928233; t_2 = 1.44400122; t_3 = 0.588363298$
B = 4	$f_4 = y_0 + a_1 e^{-(x-x_0)/t_1} + a_2 e^{-(x-x_0)/t_2} + a_3 e^{-(x-x_0)/t_3}$ $y_0 = -0.027410552; x_0 = 6.294999999$ $a_1 = 0.2086686; a_2 = 0.532550464; a_3 = 0.237164031$ $t_1 = 7.125517874; t_2 = 1.401282508; t_3 = 0.589069151$
B = 8	$f_8 = y_0 + a_1 e^{-(x-x_0)/t_1} + a_2 e^{-(x-x_0)/t_2} + a_3 e^{-(x-x_0)/t_3}$ $y_0 = -0.005391654; x_0 = 6.26$ $a_1 = 0.194515895; a_2 = 0.538869589; a_3 = 0.223472407$ $t_1 = 0.532865485; t_2 = 1.271982504; t_3 = 5.146749917$

B = 12	$f_{12} = y_0 + a_1 e^{-(x-x_0)/t_1} + a_2 e^{-(x-x_0)/t_2} + a_3 e^{-(x-x_0)/t_3}$ $y_0 = -0.013366598; x_0 = 6.231$ $a_1 = 0.54399839; a_2 = 0.223164865; a_3 = 0.196428683$ $t_1 = 1.270137; t_2 = 5.568462962; t_3 = 0.525599692$
B = 16	$f_{16} = y_0 + a_1 e^{-(x-x_0)/t_1} + a_2 e^{-(x-x_0)/t_2} + a_3 e^{-(x-x_0)/t_3}$ $y_0 = 0.011451097; x_0 = 6.206$ $a_1 = 0.236606137; a_2 = 0.235842934; a_3 = 0.466734021$ $t_1 = 2.856972464; t_2 = 2.388818387; t_3 = 0.702493174$

## 2.5 Experimental techniques

### 2.5.1 Electrical resistivity experiment

All resistivity measurements presented in this thesis were performed at the WZI using a standard four point contact method (Fig 2.1). The current (outer) and voltage (inner) leads are thin copper wires (diameter ~ 30 μm), which are soldered to insulated copper heatsinks on the copper sample holder on one end and are mounted to the sample by conductive silver paste on the other end. The value of the contact resistance (a few Ω) is normally small enough to prevent Joule heating at the lowest temperature.

For the ac resistivity measurements, the typical value of the frequency and excitation current used in the Maglab Exa cryostat is  $f \sim 16$  Hz and  $I_{exc} \sim 1-5$  mA, respectively. For the measurements in the Heliox and Kelvinox we used a Linear Research AC Resistance Bridge model LR 700 with  $f \sim 13$  Hz and  $I_{exc} \sim 30-300$  μA or an EG&G 7265 DSP lock-in amplifier with  $f \sim 13-13000$  Hz and  $I_{exc} \sim 20-300$  μA.

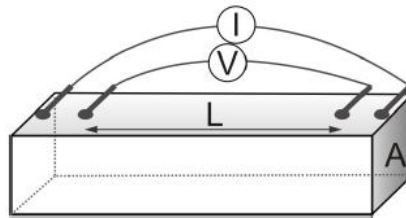


Figure 2.1 A Schematic drawing of four point contact resistivity method. In general, the distance L of the voltage contacts is ~ 1-6 mm and the cross section A varies around 1 mm<sup>2</sup>.

### 2.5.2 AC-susceptibility experiment

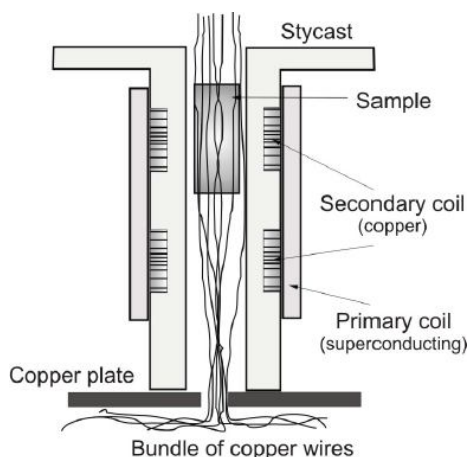


Figure 2.2 A Schematic diagram of the mutual-inductance transformer used for ac-susceptibility measurements (picture taken from Ref. 6)

Fig 2.2 shows the schematics of the mutual-inductance transformer used for ac-susceptibility measurements. The bundle of copper wires ensures a good thermal contact between the thermometer at the copper plate (not drawn) and the sample. The basic principle of operation is the following: An ac current is applied to the primary coil, which generates a small magnetic field, the driving field. The induced voltage is measured by two secondary (pick-up) coils. With an empty transformer, the signal is in principle zero since the two secondary coils are wound in opposite direction. When a sample is present in one of the coils, the magnetic field induces a magnetization, and therefore the pick-up coil signal is proportional to the ac-susceptibility. The ac-susceptibility measurements have been done using the Linear Research bridge LR700 with an excitation frequency of 16 Hz and a driving field  $\sim 10^{-5}$  T.

### 2.5.3 High pressure experiment

The hybrid piston cylinder pressure cell used for transport and ac-susceptibility experiments up to 2.5 GPa is illustrated in Fig 2.3. It is made of NiCrAl and CuBe alloys which are strong enough and nonmagnetic [7]. The inner and outer diameters are 6 mm and 25 mm, respectively. The total length of the cell varies slightly with pressure, but at the maximum pressure it is  $\sim 70$  mm. The sample space is 4.7 mm in diameter and is 8 mm long.

A hand press LCP 20 was used to pressurize the cell via a piston, which in turn pressurizes the sample via the pressure transmitting medium. A hydrostatic pressure is ascertained by using Daphne oil 7373 inside a Teflon cylinder.

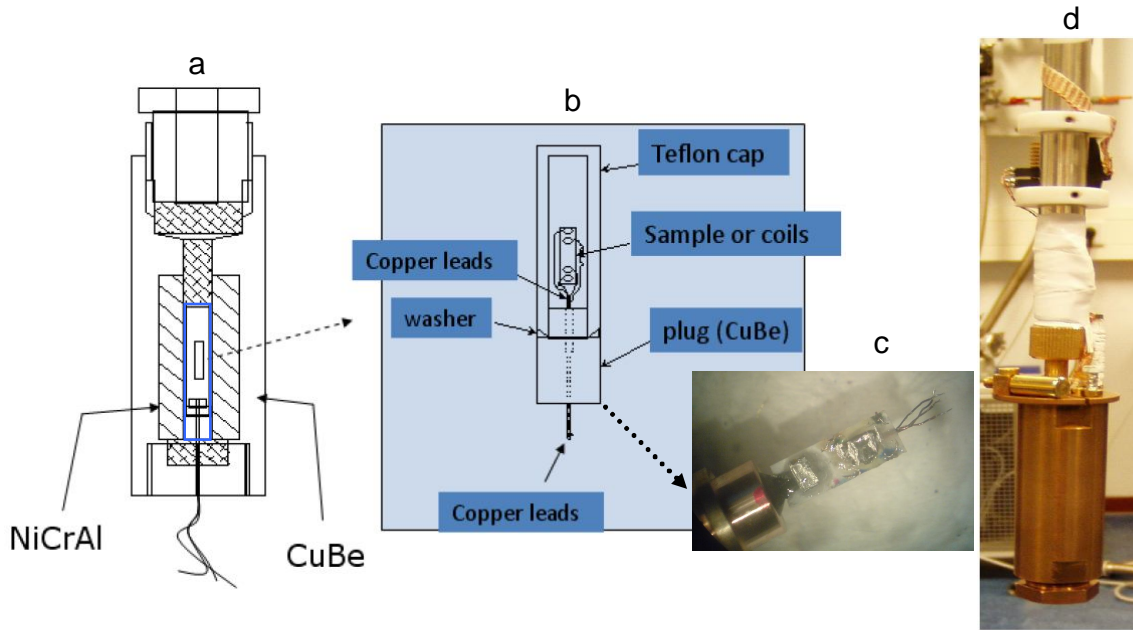


Figure 2.3 A Schematic drawing of the pressure cell and a zoom-in of the heart of the cell (a and b, taken from ref. 7). A sample and a Sn manometer supported by a paper construction on a plug (c). A complete cell at the final stage mounted in the insert of the Heliox VL (d).

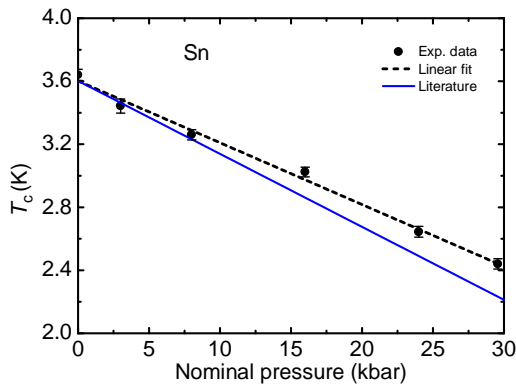


Figure 2.4 Superconducting transition temperature of Sn extracted from ac-susceptibility measurements as a function of pressure (dots) and a linear fit to the data (dashed line). The solid line presents literature data from Ref. 8.

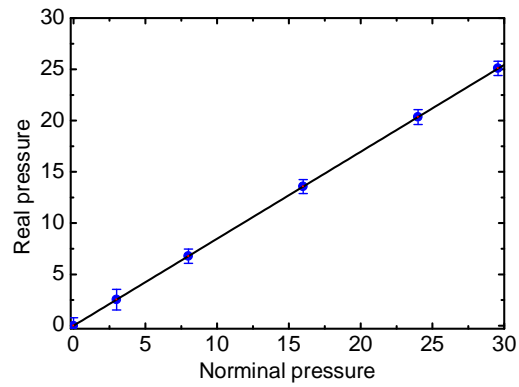


Figure 2.5 Real pressure as a function of nominal pressure. The linear fit to the data (solid line) determines the pressure cell efficiency.

Pressure calibration of the cell is done in situ by measuring the superconducting transition of a Sn sample by AC-susceptibility. Fig 2.4 presents the experimental data and a comparison to the literature to extract the actual pressure. In Fig 2.5 we show the resulting

calibration curve. Consequently, the cell efficiency is 85%, which is slightly larger than in a previous calibration (82%) [9].

#### 2.5.4 MuonSR experiment

$\mu$ SR stands for Muon Spin Rotation, Relaxation or Resonance. This technique was first developed in the late 1950s as a microscopic probe using the positive muon  $\mu^+$ . By implanting a spin-polarized muon, one at a time, into the bulk of a sample, the information obtained by detecting the resulting decay positron contains various spin-related physical properties of the investigated sample. To date it has become a powerful tool for research in condensed matter physics, such as the study of the magnetic and superconducting properties of heavy-fermion compounds [10, 11].

The  $\mu$ SR experiments have been performed using the  $\mu^+$ SR-dedicated beam line on the PSI-600MeV proton accelerator at the Swiss Muon Source of the PSI in Villigen, Switzerland. We carried out measurements at the General Purpose Spectrometer (GPS) in the temperature range above 1.5 K [4]. To attain lower temperatures (0.02-1.5 K), experiments have been performed using an Oxford Instruments top-loading  $^3\text{He}/^4\text{He}$  dilution refrigerator at the Low Temperature Facility (LTF) [5]. Samples used in these  $\mu$ SR experiments were glued to a silver holder using General Electric (GE) varnish.

#### 2.6 Data acquisition and analysis

In the different cryogenic apparatuses described above, the data obtained by various lock-in amplifiers (for example EG&G 7265 DSP), the Linear Research bridge LR700 and other devices were read by the data acquisition computers via an IEEE interface. The ORPX resistance bridge (Barras Provence) was connected to the serial port of the computers via the RS-232 protocol. To control the Heliox and Kelvinox inserts, Oxford Instruments provided standard Labview programs. In order to perform more tailor-made measurements we have improved the software, and other Labview programs have been written for data acquisition. Data files obtained from  $\mu$ SR experiments were produced by the PSI Bulk- $\mu$ SR time-differential data acquisition programme with extension ".bin" and 512 bytes/records and IEEE real-data format.

Several software packages have been used for data analysis in this work such as: Origin Pro, Mathematica (Wolfram Research), NovelLook and Wimda.

**References**

- [1] Oxford Instruments, Heliox VL, <http://www.oxford-instruments.com/>.
- [2] Oxford Instruments, Kelvinox MX100, <http://www.oxfordinstruments.com/>.
- [3] <http://neel.cnrs.fr/>.
- [4] <http://lmu.web.psi.ch/facilities/gps/gps.html>.
- [5] <http://lmu.web.psi.ch/facilities/ltf/ltf.html>.
- [6] Z. Koziol, Ph.D Thesis (University of Amsterdam, 1994) unpublished.
- [7] T. Naka, private communication.
- [8] L. D. Jennings et al., *Phys. Rev.* **112**, 31 (1958).
- [9] E. Slooten, Master Thesis (University of Amsterdam, 2009) unpublished.
- [10] A. Amato, *Rev. Mod. Phys.* **69**, 1119 (1997).
- [11] S.J. Blundell, *Contemporary Physics* **40**, 175, (1999).